AD-A087 861 FOREIGN TECHNOLOGY DIV WRIGHT-PATTERSON AFB OH F/G 11/6
FLOW STRESS OF POLYCRYSTALLINE OF ALPHA TITANIUM IN DEPENDENCE --ETC(U)
DEC 78 A DZIADON, A LATKOWSKI
UNCLASSIFIED FTD-ID(RS)T-1596-78 NL

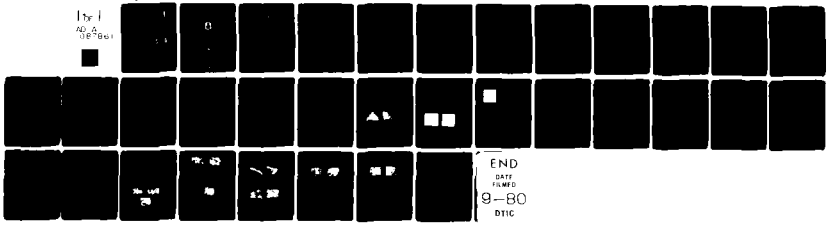

END
DATE FILMED
9-80
DTIC

PHOTOGRAPH THIS SHEET

ADA087861

DTIC ACCESSION NUMBER

LEVEL

INVENTORY

FTD-ID(RS)T-1596-78

DOCUMENT IDENTIFICATION

DISTRIBUTION STATEMENT A
Approved for public release;
Distribution Unlimited

DISTRIBUTION STATEMENT

ACCESSION FOR	
NTIS	GRA&I
DTIC	TAB
UNANNOUNCED	
JUSTIFICATION	
BY	
DISTRIBUTION /	
AVAILABILITY CODES	
DIST	AVAIL AND/OR SPECIAL
A	

DISTRIBUTION STAMP

DTIC
ELECTE
AUG 15 1980
D

DATE ACCESSIONED

DATE RECEIVED IN DTIC

PHOTOGRAPH THIS SHEET AND RETURN TO DTIC-DDA-2

DOCUMENT PROCESSING SHEET

DTIC FORM OCT 79 70A

FTD-ID(RS)T-1596-78

FOREIGN TECHNOLOGY DIVISION

FLOW STRESS OF POLYCRYSTALLINE OF ALPHA TITANIUM IN DEPENDENCE OF THE STRUCTURE AND DEFORMATION CONDITIONS

by

A. Dziadon, A. Latkowski

EDITED TRANSLATION

FTD-ID(RS)T-1596-78 15 December 1978

MICROFICHE NR: FTD-78-C-001762

FLOW STRESS OF POLYCRYSTALLINE OF ALPHA TITANIUM IN DEPENDENCE OF THE STRUCTURE AND DEFORMATION CONDITIONS

By: A. Dziadon, A. Latkowski

English pages: 27

Source: Archiwum Hutnictwa, Vol. 22, Nr. 3, 1977, pp. 469-487.

Country of origin: Poland
Translated by: SCITRAN
F33657-78-D-0619
Requester: FTD/PHE

PREPARED BY:

TRANSLATION DIVISION
FOREIGN TECHNOLOGY DIVISION
WP-AFB, OHIO.

FLOW STRESS OF POLYCRYSTALLINE OF ALPHA TITANIUM IN DEPENDENCE OF THE STRUCTURE AND DEFORMATION CONDITIONS

ANDRZEJ DZIADOŃ, ANDRZEJ ŁATKOWSKI

The paper concerns the investigations of the mechanism of polycrystalline deformation of alpha titanium in the temperature range of 25–600 °C. The experiment was carried out on iodide titanium containing 0.4% the value is given in terms of equivalent oxygen content of interstitial contaminations. The mean size of the circular flat grain of this substance was within the range of 8.7 to 170 μm.

It was found that the temperature influence on the values of actual stresses in titanium is in good agreement with the Seeger model. On the basis of the tension test the coefficients k and σ_0 taken from the Hall-Petch equation have been derived. The analysis of these coefficients shows that the initiation process of plastic deformation has specific qualities which distinguish the momentum of plastic deformation from further course of polycrystal deformation.

The observations of structure dislocations which were carried out on samples deformed at a rate of $\dot{\epsilon} = 3.6 \times 10^{-4}\ s^{-1}$ allow to state that the dislocations cause tangles formation inside grains; systems of simple dislocations have been also observed. At a temperature of 300°C the deformation caused formation of cellular structure. At the grain boundary the pile-up was not found, whereas in case of microdeformations at the grain boundary emission of partial dislocations has been observed.

On the basis of the changes of the coefficients k and σ_0 from the Hall-Petch equation versus rate of deformation and on the basis of carried out observations of dislocation structures the authors suggest that in the investigated temperature range the initiation process of plastic deformation of alpha polycrystalline titanium can be described by means of the Li model.

1. Introduction

The role of one of the parameters characterizing the structure, which is the grain size, on the stress value causing the plastic deformation of polycrystal can be expressed analytically by the Hall-Petch equation [1,2]:

$$\sigma = \sigma_0 + k d^{-1/2}$$

where σ - the stress causing the given plastic deformation, σ_0 - the stress necessary to overcome the "friction" to which the moving dislocations are subjected in the crystal lattice, k - constant representing the resistance to the spreading of slide zone, d - grain diameter.

It was experimentally confirmed, that the above relation is satisfied by the alpha titanium, both in the pull test [3,4,5] and the hardness measurements [6,7,8]. The Hall-Petch relation for the alpha titanium is interpreted in the literature by the Conrad model [9]. Such a description of the polycrystal deformation process is only a formal description taking into account only the determined qualitative relation between the stress increase and the increase of dislocation density. In turn, the dislocation density depends on the grain size. In this way one can make a direct connection between the stress value and the grain size.

The mechanism of polycrystalline deformation in alpha titanium, used especially the process of deformation initiation, is still unexplained. It is suggested that the deformation initiation takes place through the dislocation generation of the grain boundary [8], but at the same time one

doesn't exclude the possibility of deformation propagation due to the pile-ups [4].

The still incomplete state of experimental data and their controversial interpretations were the reasons for undertaking this work of studying the crystalline deformation of alpha titanium in wide temperature range from 25°C to 600°C. The goal of this study was the attempt to determine the mechanism of plastic polycrystalline deformation of alpha titanium with the emphasis on initiation of this deformation. The experimental method used, was the analysis of Hall-Petch relation as a function of deformation for the given temperature range, together with the observation of dislocation structure changes.

2. Experimental material and method

The studied material was the iodine titanium made by the Titanium Imperial Chemical Industries. The amount of interstitial admixture was equivalnet to 0.4 atomic percent of oxygen (according to: N = 20, C = 3/4 O [10]).

The initial material, the roll stock 10 mm in diameter, was pulled without heating with the cumulative deformation factor of 70%. The samples made of it were 3.6 mm in diameter and 23 mm length and were heated to recrystalize in copper containers (Table 1).

The pulling tests were performed at temperature range from 25° to 600°C, using the strain testing machine "Instron", equipped with high temperature, three-range oven with the argon atmosphere. To extend the range of testing, two deformation speeds were applied: $\dot{\varepsilon} = 3.6 \times 10^{-4}$ sec^{-1} and $\dot{\varepsilon} = 1.5 \times 10^{-2} sec^{-1}$.

The microscopic studies were performed using the "Neophot - 2" optical microscope and the "Tesla" BS - 613 electron microscope. The

texture studies were made using the X-ray method and the TUR 60 machine.

3. Experimental results.

3.1 The structure of heated alpha titanium

As a result of heating, five groups of samples were obtained, differing in grain size (Table 1). It was determined that the grains are uniformly distributed and have the even axis character in each group. The grain size was determined using the Jeffries - Saltykov method as quoted by Rys (11), as the "average diameter of flat circular grain". The measurements were made on the polished cuts along and across the sample to be pulled.

The observation of thin foils allowed to determine, that the grain interiors and their boundaries are free from fractioning. A typical picture of grain boundary is shown in Fig 1. Inside the grains, the simple dislocation systems were found, typical to the heated material (Fig 2). The X-ray studies indicate the existence of $(1\ 0\ \bar{1}\ 0)$ structure in recrystallized titanium. Fig 3 shows the example of X-ray diffraction obtained from a sample with 17.5 μm grain.

The slip in alpha titanium is most likely in (10$\bar{1}$0), $[\ 12\bar{1}0]$, and$(10\bar{1}1)$ $[12\bar{1}0]$ systems. The dislocations in these planes are the "tree" dislocation for the(0001) plane. Thus to determine the slip dislocation density, one has to determine the density of etched cavities in the (0001) plane. From the structure studies it follows, that the (0001) plane is parallel or only slightly deviating from the sample axis. This is why the etching was done in the samples axial planes. In reality, it turns out that both, in fine and coarse grained material, only few grains had the etching cavities. Cass [12] determined, that the etching of dislocation cavities in the (0001) titanium plane takes place only if

this plane forms the angle with the cut plane not larger than a few degrees. Figures 4 and 5 show the cavities in grains with the average diameters of 17.5 and 64.0 μm. Fig 4 shows also the etching shape of the (0001) plane. The dependence of "average dislocation density", that is, the average number of dislocations per surface unit, on the "average circular diameter of flat grain" is shown in Fig 6.

Summing the above results concerning the structure of the test material, one has to emphasize, that as a result of recrystallization one obtained both types of samples, fine and coarse grained. That required operation within a wide range of times and heating temperatures. One has to assume, that the change of thermal processing parameters could have influence on a structure of grain boundaries and cause the differences in a degree of separation of interstitial admixture atoms to the grain boundaries and dislocations. These structural changes are always connected with the recrystalization process. With the increase of average grain diameter the dislocation density inside the grain decreases, and the dislocation density is of the order of 10^6 cm^{-1}. The recrystalization twins or the polygonal systems were not found in the heated material. It also didn't contain any fractionation inside or on the grain boundaries. This is why it can be treated as a single phase alloy.

3.2 The effect of the grain size and temperature on the stress values.

The dependence of the stress on temperature and degree of deformation are shown in Figs 7 and 8 for the fine and coarse grained material. To separate this functional dependence from the changes of elasticity modulus with temperature, the measured stresses were divided by the titanium cross sectional elasticity modulus G for the given temperature [13].

From the curves it can be seen that it is possible to divide the temperature range 25° - 600°C into two regions: in the first one the stress is very sensitive to the temperature changes, in the second one the temperature has no effect on the stress. In Figs 7 and 8 the first region extends to about 250°C. The increase of deformation speed by two orders of magnitude caused the extension of the first region to about 400°C (Figs 9 and 10). The dependence between the stress and temperature is then in agreement with the classical Seeger model [14], which assumes that in the case of thermally activated dislocation movement, the stress depends not only on the dislocation structure, but also on temperature and deformation speed.

The Hall-Petch graphs were made for the stresses corresponding to the deformations $\varepsilon = 0.0002$, $\varepsilon = 0.02$, $\varepsilon = 0.04$, $\varepsilon = 0.08$ and $\varepsilon = 0.16$. These dependences, for the deformation speeds $\dot{\varepsilon} = 1.5 \times 10^{-2} sec^{-1}$ and $\dot{\varepsilon} = 3.6 \times 10^{-4} sec^{-1}$ are presented for 200°C temperature in Fig 11. The values for the k and σ_0 coefficients in Hall-Petch equation, obtained by least-square fitting, are shown in Tables 2 and 3. As it can be seen (Fig 11, Table 2 and 3) that the values of directional coefficient k and "friction resistance" σ_0 depend on the deformation degree and temperature. These relations are summarized in Figs 12 through 15. They show (Fig 12 and 13), the dependence of k coefficient as a function of deformation, and (Fig 14 and 15) the temperature dependence of σ_0/G coefficient, for the deformation speeds $\dot{\varepsilon} = 1.5 \times 10^{-2}$ sec^{-1} and $\dot{\varepsilon} = 3.6 \times 10^{-4}$ sec^{-1} respectively.

3.3 Structural studies

The observations of dislocation structure were conducted on the samples with the average grain diameters 8.7 μm and 170.0 μm, deformed with the speed $\dot{\varepsilon} = 3.6 \times 10^{-4}$ sec^{-1} at temperatures 25°C and 300°C. The deformations

of these samples at 25°C were $\epsilon = 0.01$, $\epsilon = 0.04$ and $\epsilon = 0.08$, and at 300°C: $\epsilon = 0.02$, $\epsilon = 0.04$ and $\epsilon = 0.08$. The fine grained samples exhibited definite plasticity limit. The deformation values $\epsilon = 0.01$ and $\epsilon = 0.02$ were for these samples at the end of the stretching plateau.

Fig 16 shows the characteristic dislocation structures of titanium for the $\epsilon = 0.01$ deformation at 25°C, and Fig 17 the structure at $\epsilon = 0.02$ at 300°C temperature. The pictures show, that the structure is characterized by the tangles (Fig 16a and 17) or by a simple dislocation systems (Fig 16b and 16c), no pile-ups were detected. A quite similar type of structure was observed in coarse grained material (Fig 18 and 19). The grain boundary seen in Fig 19 is almost perpendicular to the surface of thin foil; in Fig 18 it forms a sharp angle with it. Fig 16 shows also the dislocation dipoles. At the same time the interaction between the dislocation and the grain boundary was observed (Fig 16c).

At the end of the stretching graph plateau the state of titanium deformation is so advanced, that it is difficult to separate the process of pure dislocation generation at the grain boundary from the changes related to the fact that it also forms an obstacle for the arriving dislocations. Moreover, at this deformation state the dislocation interact with each other inside the grain, which additionally complicates the interpretation. To obtain the clarity of structural changes related to the initiation of plastic deformation process, the microscopic observations should be conducted for much smaller deformations. In connection with that, the attempt was made to observe the thin foils after microdeformations. A thin foil of heated, fine grained titaniur was placed in the electron microscope, the electron beam was focused on it and at the same time the beam intensity was increased. This caused the microdeformations due to the local heating. The structural changes associated with such microdeformations are shown in Fig 20.

An increase of the deformation to $\varepsilon = 0.04$ causes an increase in dislocation density, which form the characteristic tangles. This is shown as an example in Fig 21. The further deformation at 25°C doesn't change the structure character, only the dislocation density increases (Fig 22).

On the other hand, the deformation beyond the stretching graph plateau lead to the formation of cellular structure at 300°C. The formation of cellular structure was quite viable at $\varepsilon = 0.04$, both for the grain size 8.7 μm (Fig 23) and for the 170.0 μm grain (Fig 24). For the deformation with $\varepsilon = 0.08$ the cellular structure is well established, which can be seen in Figs 25 and 26.

4. Discussion

The Figs 7 through 10 show the typical influence of temperature, deformation, deformation speed and the grain size on the actual value of stress divided by the cross sectional elasticity modulus. In the functional dependence of σ/G with temperature one can separate the thermal and athermal components of σ/G. During the deformation with the speed of $\dot{\varepsilon} = 3.6 \times 10^{-4} sec^{-1}$ the value of σ/G starting at 250°C doesn't change for the given deformation and grain size. One can then consider this constant value a thermal one. At temperatures lower than 250°C the total σ/G value may be treated as a sum of two components; thermal and athermal. The increase of deformation speed by two orders of magnitude moves the range of stress thermal component to about 400° C. Simultaneously one observes the disappearance of straight-line section of σ/G-T plot at higher deformations. This is caused by the fact that with the increase of deformation the free path between the barriers in the crystal lattice decreases, which combined with the deformation speed, creates a less favorable condition for

the thermal dislocation activation to pass these barriers.

A similar dependence on temperature and deformation speed is observed for the σ_i coefficient in Hall-Petch effect, called the "friction resistance" (Fig 14 and 15). In titanium with the $(10\bar{1}0)$ structure the slip may take place in the prismatic system $(10\bar{1}0)\left[\bar{1}2\bar{1}0\right]$ or in the piramid system $(10\bar{1}1)\left[\bar{1}2\bar{1}0\right]$ (15). The small difference between the critical stresses in these systems causes that the slip within the studied temperature range is possible in both systems. Dislocations in the prismatic system are the "forest" dislocations in the piramid system and reverse. The increase of slip dislocation density in one of these systems causes the increase of "forest" dislocations in the other. This causes the decrease of distances between the barriers which can be overcome by the thermal activation. The increase of deformation speed decreases the probability that the dislocation obtains the additional energy through thermal fluctuation, sufficient to overcome this barrier.

Another characteristic property of σ/G -T plots is a large difference between the stress values corresponding to the deformations $\varepsilon = 0.002$ and $\varepsilon = 0.02$ in coarse grained titanium (Fig 8 and 10) in relation to the fine grained titanium (Figs 7 and 9). Similarly, there is a large difference between the values of σ_i coefficient in Hall-Petch equation for deformations $\varepsilon = 0.002$ and $\varepsilon = 0.02$ (Fig 14 and 15). A large increase in σ_i/G value in early stage of deformation, higher than in the following deformation course, can be associated with the considerable increase of dislocation density at this stage of deformation as was observed by Jones and Conrad [4]. The increase of σ/G at the transition from $\varepsilon = 0.002$ to $\varepsilon = 0.02$ shows the stress increase caused by this dislocation density increase. In the coarse grained material (Fig 8 and 10) this difference in stresses

is very large. At the same time, much higher [4] increase of dislocation density in the grained material causes negligible stress increase (Fig 7 and 9). One can see, that there is a factor causing the increase of plastic deformation "start" stress in polycrystal, with the decrease of grain size.

The full picture of this phenomenon is given by the analysis of changes of k coefficient in Hall-Petch equation during the deformation process.

It was determined, that in the entire range of temperatures from 25°C to 500° C (at 600 °C the Hall-Petch relation was not satisfied due to the recrystallization) the values of k coefficient determined for the deformation ε = 0.002, which corresponds to the beginning of plastic deformation, are much higher that the values of these coefficients for ε = 0.02 (Fig 11, Table 2 and 3). From the data in Table 2 and 3, one can see that the values of k for ε = 0.002 are about twice as high than the k values for ε = 0.02. Next, with the increase at the deformation, the values of k begin to increase reaching at few tens of percent deformations the initial values. That is graphically presented in Fig 12 and 13. One can see, that the character of k value changes as a function of deformation was identical for all temperatures and deformation speeds.

Jones and Conrad (4) while studying the iodine titanium with the interstitial admixture equivalent to 0.09% of oxygen, determined that the k coefficient in Hall-Petch relation reaches the value of 0.48 kG/ mm $^{3/2}$ at ε = 0.002, and doesn't change with additional deformation.

Comparing these data, which were obtained for the high purity material, obtained by the method of zone melting, with the present results, one has to conclude, that the changes of k coefficient as a function of deformation is primarily determined by the chemical composition, or more precisely, the amount of interstitial admixtures.

Similar observation were made by Gupta and Garofalo [16]. The ions studied by them, indicated a very high value of k_y (the k value for the lower plasticity limit) as compared with the value of k in the Hall-Petch relation obtained for $\varepsilon = 0.05$ deformation. By reducing the number of interstitial admixtures, they obtained the state in which the k value reached the minimum for the entire range of studied deformations (up to $\varepsilon = 0.15$).

One can assume with Cottrell [17], that the interstitial atoms diffuse towards the dislocation sources and block them. From the present results it follows, that in titanium the blocking of dislocation sources by interstitial admixture atoms is in close relation with the grain size: the smaller the grain the larger is the blocking effect.

One could ask now how the dislocation sorces are unblocked and where these sources are located.

From the point of view of theoretical analysis of Hall-Petch relation, it is possible to accept both, the Li model of dislocation emission from the grain boundary [18], and the Cottrell model [19] which is a modification of pile-up model assuming the initiation of deformation by unblocking the sources inside the grains due to the dislocation pile-ups. On the one hand, the decrease of average grain diameter may be connected with the decreased distance between grains. This causes the increase of pile up stresses, which in turn will cause on the grain boundary the stress concentration sufficient to unblock the source in the neighboring grain. On the other hand, the decrease of grain diameter causes the severalfold increase of grain boundary surface in the fine grained material as compared with coarse grained. To this grain boundary surface the interstitial admixture atoms diffuse from the grain interior.

The problem of admixture atoms diffusion to the boundaries described by Westbrook [20]. Several papers were devoted to the separation of inter-

stitial atoms on grain boundaries. Among them, Phillips [21] experimentally determined the diffusion of carbon atoms to the grain boundaries in iron, Latanision and Opperhauser [22] the separation of hydrogen on grain boundary in nickel, and Walsh and Kear [23] the separation of boron in nickel alloy. Fortes and Ralph [24] using the ion microscope, determined the quantitative change of oxygen concentration in iridium grain as a function of distance from grain boundary. The oxygen concentration on the grain boundary was six times higher than in the interior, and the separation region was about 450 Å.

In view of these experiments one can assume, that in the titanium lattice there is also a separation towards the grain boundary, most of all for the mobile interstitial atoms.

In connection with that, the effect of large stress differences in fine and coarse grained material at the point of deformation initiation (ε = 0.002), larger than for subsequent deformation, can be connected with the unblocking of dislocation sources on the grain boundaries. Assuming according to the Li model (18), the same density of potential dislocation sources on the grain boundary, the total number of sources on grain boundary will be much higher in fine grained material. The high value of k coefficient in Hall-Petch relation for ε = 0.002 results from unblocking of larger number of sources as finer grained the material is. The observations of dislocation structure support this model. One doesn't observe in the studied material, flat dislocation systems forming the pile-up on the grain boundaries. At small deformations, both in room and elevated temperatures the dislocation angles form, and at 300°C one observes at ε = 0.04 the formation of cellular structure. The dislocation systems observed at ε = 0.01 and at room temperatures (Fig 16) are not diffuse, and lead to speculation that they are formed as a result of

generation taking place from the grain boundary. Finally, for the micro-deformations one observed the cases of dislocation emission from the grain boundary with the formation of location error. Similar effect of partial dislocation emission from the grain boundary under the influence of the electron beam was observed by Murr [25] on thin stainless steel foils.

Number of authors suggest that polycrystal deformation is initiated on the grain boundaries.

Warthington and Smith [26] and Corrington and McLean [27] using the cavity etching method,experimentally determined the dislocation generation from the grain boundary during the microdeformation of iron-silicon alloy (3 - 4% Si). Edigton and Smallman [28] observed the dislocation systems, during the vanadium microdeformation, similar to Fig 16c, and interpreted them as an effect of source activities on grain boundary. Van Thorne and Thomas [29] using the analysis of niobium dislocation structure suggest, that the dislocation sources in the microdeformation phase are the grain boundaries and the seperated atoms. Mascanzoni and Buzzichelli [30] on the basis of observation of grain boundaries in pure alpha iron, suggest the existence of Frank-Read sources on boundaries. Thomson [31] on the basis of studies of grain boundaries in nickel subjected to small deformation ($\varepsilon = 0.002$) suggests that the observed loops could be the dislocation sources.

According to the classical Li model [10], the dislocation generation from the grain boundaries takes place only in the initial deformation stage. The further increase of dislocation density is realized by the sources acting inside the grain. The grain boundaries limit the dislocation movement. This shows up in the systematic increase of k coefficient with the deformation increase, starting with $\varepsilon = 0.02$, and also in the changes

of dislocation structure. The thin foils in addition to the considerable increase of dislocation density, show the concentration of dislocations on the grain boundaries and the interaction of lattice dislocation with these boundaries. Similar increase of k coefficient, after reaching the local minimum was determined among others by Coleman and Hardie [32] on zirconium and Omar and Entwisbe [33] for niobium.

As a consequence of conducted studies and the above discussions, it is justified to propose the description of polycrystalline deformation of alpha titanium by the Li model of dislocation operation from the grain boundary.

#

Bibliography

[1] E. O. Hall, Proc. Phys. Soc. B 64, 742 (1951).
[2] N. J. Petch, J. Iron Steel Inst. 174, 25 (1953).
[3] K. Okazaki, H. Conrad, Acta Met. 21, 1117 (1973).
[4] R. L. Jones, H. Conrad, Trans. of AIME 245, 779 (1969).
[5] G. Sargent, H. Conrad, Scripta Met. 3, 43 (1969).
[6] H. Hu, R. C. Cline, Trans. of AIME 242, 1013 (1968).
[7] R. W. Armstrong, Met. Trans. 1, 1169 (1970).
[8] K. Okazaki, N. Conrad, Trans. Japan Inst. Met. 14, 364 (1973).
[9] H. Conrad, S. Feuerstein, L. Rice, Mat. Sc. and Eng. 2, 157 (1967).
[10] H. Conrad, Acta Met. 14, 1631 (1966).
[11] J. Ryś, Wstęp do metalografii ilościowej, (Introduction to quantitative metalography) „Śląsk" Katowice, 1970.
[12] T. R. Cass, Trans. of AIME 239, 1864 (1967).
[13] F. Girard, G. Vidal, Revue de Metallurgie MS 2, 118 (1960).
[14] A. Seeger, Z. Naturforsch 9a, 759, 819 856 (1954).
[15] A. Łatkowski, Archiwum Hutnictwa t. XIII, z. 3, 273 (1968).
[16] I. Gupta, F. Garofalo, Mat. Sc. and Eng. 5, 271 (1969/70).
[17] A. H. Cottrell, B. A. Bilby, Proc. Phys. Soc. 62A, 49 (1949).
[18] J. C. M. Li, Trans. Metall. Soc. of AIME 227, 239 (1963).
[19] A. H. Cottrell, Trans. of AIME 212, 192 (1958).
[20] J. H. Westbrook, Met. Rev. 9 nr. 36, 415 (1964).
[21] V. A. Phillips, Acta Met. 11, 1139 (1963).
[22] R. M. Latanision, H. Opperhauser, Met. Trans. 6A, 233 (1975).
[23] J. M. Walsh, B. H. Kear, Met. Trans. 6A, 226 (1975).
[24] M. A. Fortes, B. Ralph, Acta Met. 15, 707 (1967).
[25] L. E. Murr, Met. Trans. 6A, 505, (1975).
[26] P. J. Worthington, E. Smith, Acta Met. 12, 1277 (1964).
[27] W. E. Carrington, D. Mc Lean, Acta Met. 13, 493 (1965).
[28] J. W. Edington, R. E. Smallman, Acta Met. 12, 1313 (1964).
[29] L. I. van Torne, G. Thomas, Acta Met. 11, 881 (1963).
[30] A. Mascanzoni, G. Buzzichelli, Phil. Mag. 22, 857 (1970).
[31] A. W. Thompson, Acta Met. 23, 1337, 1975.
[32] C. E. Coleman, D. Hardie, J. Inst. of Metals 94, 387 (1966).
[33] A. M. Omar, A. R. Entwisle, Mat. Sc. and Eng. 5, 263 (1969/70).

Table 1

Heating conditions and obtained grain size

1 - temperature, 2 - heating time, 3 - the diameter of circular flat grain.

(1) Temperatura °C	(2) Czas wygrzewania min.	(3) Średnia średnica kołowego ziarna płaskiego µm
650	15	8,7
680	10	17,5
680	20	31,7
750	25	84,0
825	150	170,0

Fig. 1

Fig. 2

Fig 1. Grain boundary in a sample with the average grain size of 8.7 µm.

Fig 2. Dislocation structure in the sample with the average grain size of 8.7 µm.

Fig 3. X-ray diffractogram of heated wire with the fine grained structure (d = 17.5 μm).

Fig 4. etching cavities in (0001) plane.

grain diameter 17.5 μm. Magnification 1600X

Fig. 3

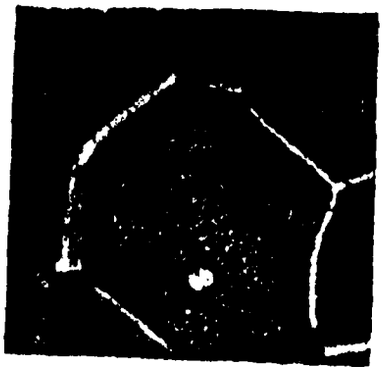

Fig. 4

Fig. 5

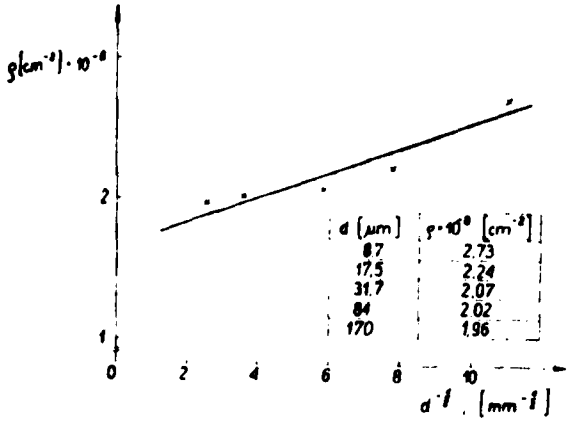

Fig. 6

Fig 5. Etching cavities in (0001) plane

Grain diameter 84.0 μm. Magnification 1000X.

Fig 6 Dislocation density crossing the (0001) plane as a function of grain size.

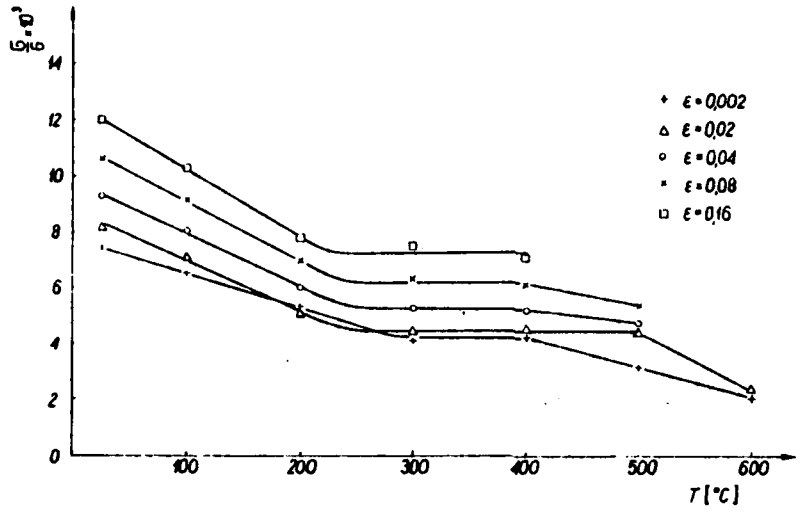

Fig 7. Influence of temperature on σ/G value for titanium with the average grain size 8.7 μm. Deformation speed $\dot{\varepsilon} = 3.6 \times 10^{-4} sec^{-1}$.

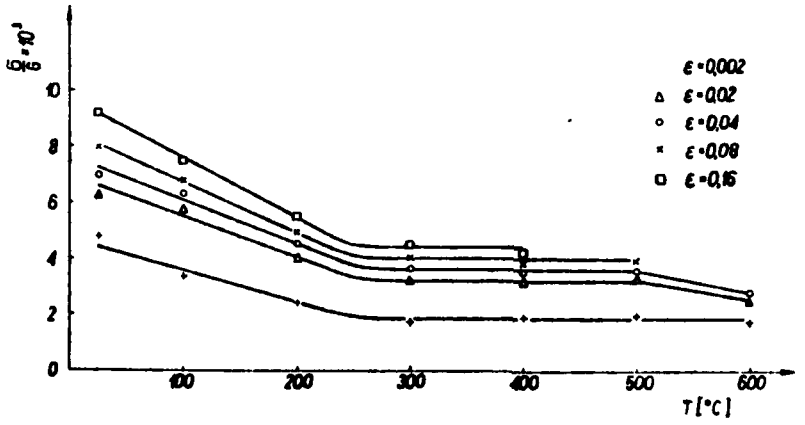

Fig 8. Influence of temperature on σ/G value for titanium with the average grain size 170.0 μm. Deformation speed $\dot{\varepsilon} = 3.6 \times 10^{-4} sec^{-1}$.

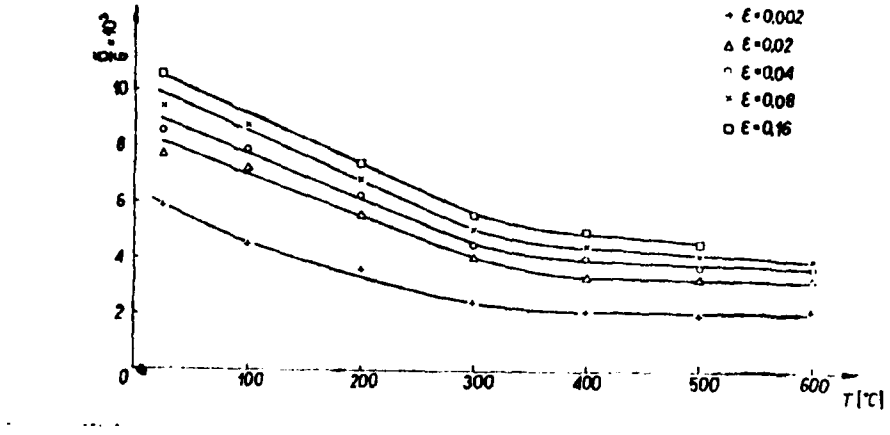

Fig 9. Temperature dependence of σ/G value for titanium with the grain size 8.7 μm. Deformation speed $\dot{\varepsilon} = 1.5 \times 10^{-2} sec^{-1}$.

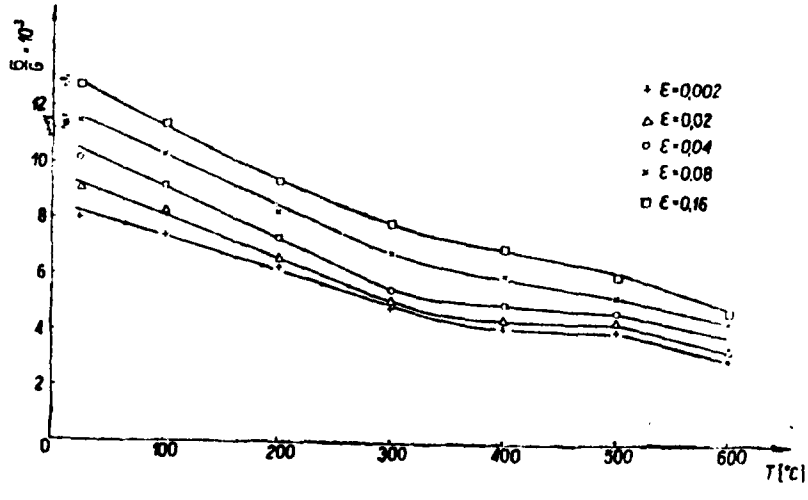

Fig 10. Temperature of σ/G value for titanium with the grain size 84.6 μm. Deformation speed $\dot{\varepsilon} = 1.5 \times 10^{-2}$ sec^{-1}.

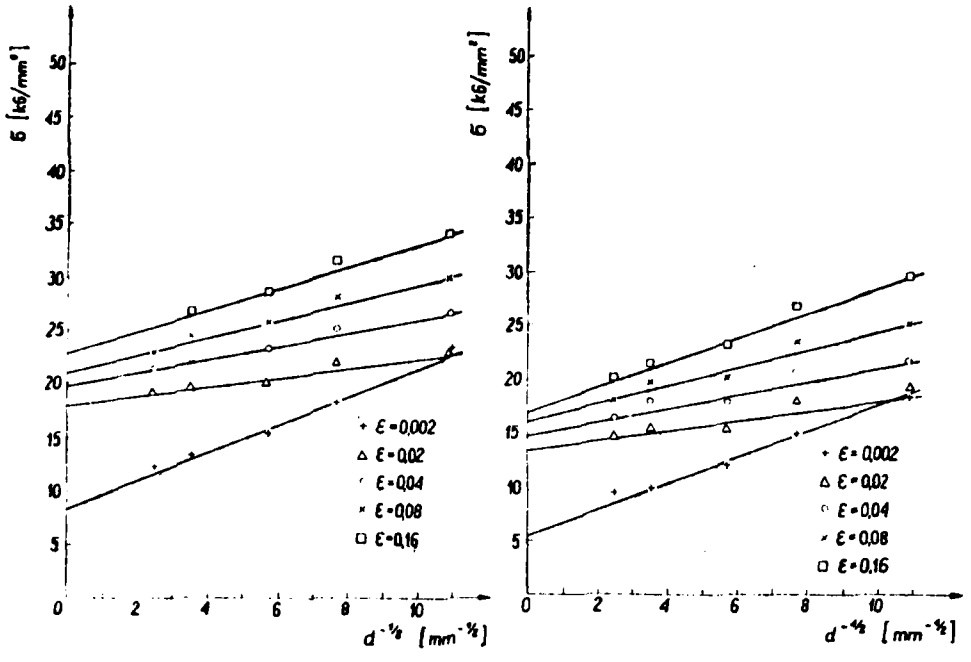

Fig 11. Hall-Petch relation for the 200°C temperature. Deformation speed $\dot{\varepsilon} = 1.5 \times 10^{-2}$ sec^{-1} (left side) and $\dot{\varepsilon} = 3.6 \times 10^{-4}$ sec^{-1} (right side).

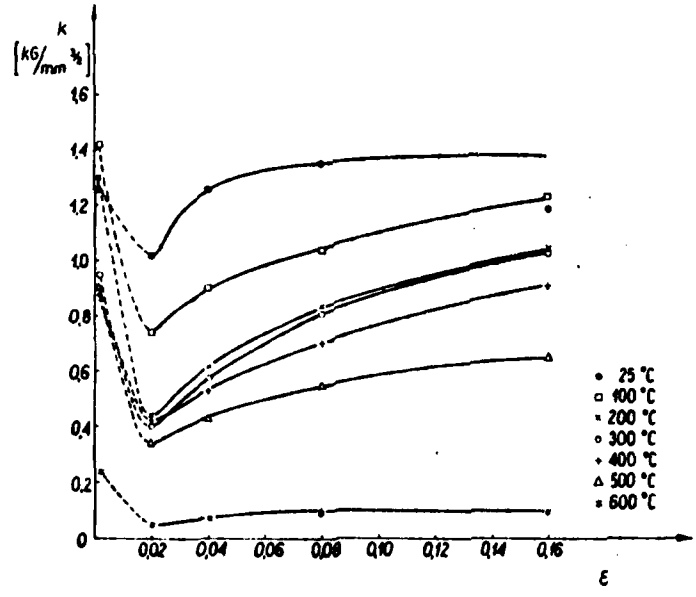

Fig 12. Influence of deformation ratio on k coefficient value. Deformation speed $\dot{\varepsilon} = 1.5 \times 10^{-4}$ sec^{-1}.

Table 2. The values of k and σ_0 coefficients in the Hall-Petch relation together with their standard deviations S_k and S_{σ_0} and the correlation coefficients R. Deformation speed $\dot{\varepsilon} = 1.5 \times 10^{-2}$ sec^{-1}.

Temp. °C	k	S_k	σ_0	S_{σ_0}	R	k	S_k	σ_0	S_{σ_0}	R
	$\varepsilon = 0{,}002$					$\varepsilon = 0{,}02$				
25	1,26	0,15	18,4	1,0	0,89	1,02	0,23	26,5	1,5	0,93
100	1,42	0,10	12,6	0,7	0,99	0,74	0,16	23,8	1,1	0,94
200	1,30	0,09	8,3	0,6	0,99	0,44	0,07	17,8	0,4	0,97
300	0,94	0,04	6,2	0,2	0,99	0,40	0,04	14,5	0,2	0,99
400	0,88	0,07	3,5	0,4	0,99	0,43	0,02	8,6	0,1	0,99
500	0,90	0,12	2,6	0,8	0,97	0,34	0,01	7,6	0,3	0,98
600	0,25	0,16	1,0	1,1	0,64	0,05	0,17	7,1	1,1	0,18
	$\varepsilon = 0{,}01$					$\varepsilon = 0{,}08$				
25	1,26	0,26	28,9	1,7	0,94	1,35	0,18	32,7	1,2	0,97
100	0,90	0,20	26,2	1,3	0,93	1,04	0,19	29,0	1,3	0,95
200	0,61	0,05	19,6	0,3	0,99	0,83	0,07	20,9	0,5	0,99
300	0,57	0,03	12,7	0,2	0,99	0,81	0,02	13,6	0,1	0,99
400	0,53	0,02	9,8	0,1	0,99	0,70	0,03	10,7	0,2	0,99
500	0,43	0,05	8,3	0,3	0,98	0,55	0,07	9,0	0,4	0,98
600	0,07	0,19	8,2	1,3	0,20	0,10	0,22	8,7	1,4	0,28
	$\varepsilon = 0{,}16$									
25	1,18	0,18	38,3	1,2	0,97					
100	1,23	0,14	30,8	1,1	0,99					
200	1,03	0,10	22,7	0,7	0,99					
300	1,03	0,03	14,7	0,2	0,99					
400	0,91	0,04	11,6	0,3	0,99					
500	0,65	0,09	10,1	0,6	0,98					
600	0,02	0,10	10,9	0,9	0,19					

Table 3. The values of k and σ_0 coefficients from the Hall-Petch relation together with their standard deviation S_k and S_{σ_0} and the correlation coefficients R. The deformation speed $\dot{\varepsilon} = 3.6 \times 10^{-4}\,\mathrm{sec}^{-1}$.

Temp. °C	k	S_k	σ_0	S_{σ_0}	R	k	S_k	σ_0	S_{σ_0}	R
	$\varepsilon = 0{,}002$					$\varepsilon = 0{,}02$				
25	1,17	0,24	16,6	1,6	0,94	0,68	0,29	25,2	1,9	0,80
100	1,41	0,12	9,9	0,8	0,99	0,53	0,11	21,3	0,8	0,94
200	1,24	0,09	5,4	0,6	0,99	0,47	0,12	13,3	0,8	0,92
300	0,97	0,04	3,0	0,3	0,99	0,48	0,03	9,1	0,2	0,99
400	0,84	0,11	3,0	0,7	0,98	0,33	0,02	8,7	0,1	0,99
500	0,47	0,07	4,0	0,4	0,97	0,16	0,09	9,1	0,5	0,72
600	0,17	0,08	3,6	0,5	0,75	0,02	0,10	5,7	0,7	0,09
	$\varepsilon = 0{,}04$					$\varepsilon = 0{,}08$				
25	0,89	0,31	27,8	2,1	0,85	1,04	0,27	31,0	1,8	0,92
100	0,75	0,13	23,1	0,9	0,96	1,00	0,13	24,8	0,9	0,97
200	0,64	0,12	14,7	0,8	0,95	0,86	0,11	15,9	0,8	0,97
300	0,63	0,02	10,3	0,1	0,99	0,87	0,02	11,2	0,1	0,99
400	0,47	0,02	9,3	0,1	0,99	0,63	0,03	10,0	0,2	0,09
500	0,14	0,15	10,2	1,0	0,47	0,29	0,17	10,9	1,1	0,71
	$\varepsilon = 0{,}16$									
25	1,17	0,20	35,2	1,3	0,98					
100	1,29	0,12	26,3	0,8	0,99					
200	1,18	0,08	16,8	0,5	0,99					
300	1,16	0,03	12,0	0,2	0,99					
400	0,80	0,03	10,9	0,2	0,99					

Table 3. The values of k and σ_0 coefficients from the Hall-Petch relation together with their standard deviation S_k and S_{σ_0} and the correlation coefficients R. The deformation speed $\dot{\varepsilon} = 3{,}6 \times 10^{-4}\,\mathrm{sec}^{-1}$.

Temp. °C	k	S_k	σ_0	S_{σ_0}	R	k	S_k	σ_0	S_{σ_0}	R
	$\varepsilon = 0{,}002$					$\varepsilon = 0{,}02$				
25	1,17	0,24	16,6	1,6	0,94	0,68	0,29	25,2	1,9	0,80
100	1,41	0,12	9,9	0,8	0,99	0,53	0,11	21,3	0,8	0,94
200	1,24	0,09	5,4	0,6	0,99	0,47	0,12	13,3	0,8	0,92
300	0,97	0,04	3,0	0,3	0,99	0,48	0,03	9,1	0,2	0,99
400	0,84	0,11	3,0	0,7	0,98	0,33	0,02	8,7	0,1	0,99
500	0,47	0,07	4,0	0,4	0,97	0,16	0,09	9,1	0,5	0,72
600	0,17	0,08	3,6	0,5	0,75	0,02	0,10	5,7	0,7	0,09
	$\varepsilon = 0{,}04$					$\varepsilon = 0{,}08$				
25	0,89	0,31	27,8	2,1	0,85	1,04	0,27	31,0	1,8	0,92
100	0,75	0,13	23,1	0,9	0,96	1,00	0,13	24,8	0,9	0,97
200	0,64	0,12	14,7	0,8	0,95	0,86	0,11	15,9	0,8	0,97
300	0,63	0,02	10,3	0,1	0,99	0,87	0,02	11,2	0,1	0,99
400	0,47	0,02	9,3	0,1	0,99	0,63	0,03	10,0	0,2	0,09
500	0,14	0,15	10,2	1,0	0,47	0,29	0,17	10,9	1,1	0,71
	$\varepsilon = 0{,}16$									
25	1,17	0,20	35,2	1,3	0,96					
100	1,29	0,12	26,3	0,8	0,99					
200	1,18	0,08	16,8	0,5	0,99					
300	1,16	0,03	12,0	0,2	0,99					
400	0,80	0,03	10,9	0,2	0,99					

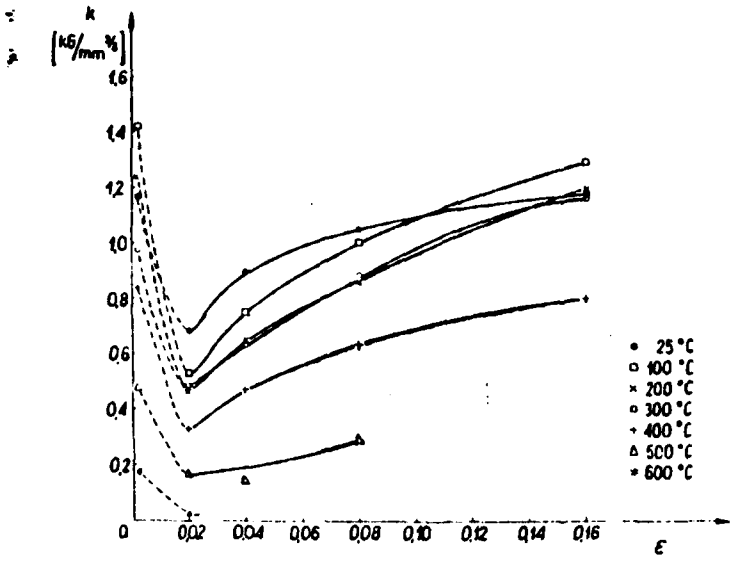

Fig 13. Influence of deformation ratio on the value of k coefficient. Deformation speed $\dot{\varepsilon} = 3.6 \times 10^{-4}\ sec^{-1}$.

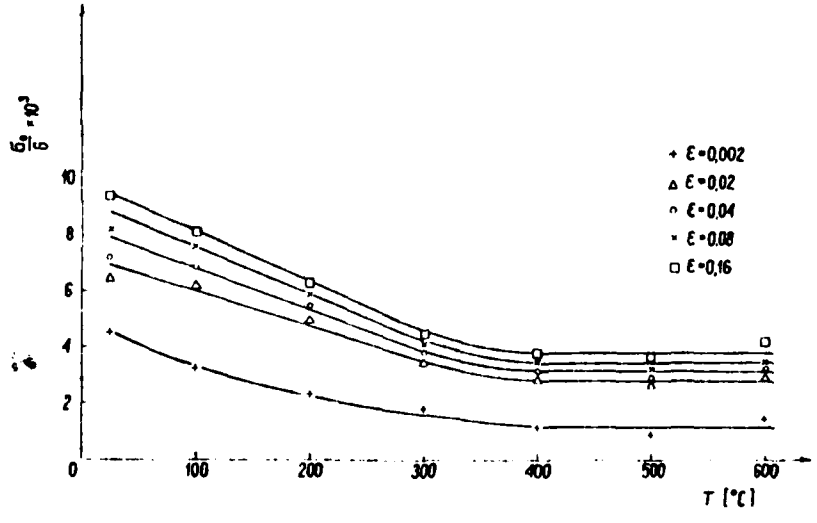

Fig 14. Temperature dependence of σ/G coefficient. Deformation speed $\dot{\varepsilon} = 1.5 \times 10^{-2}\ sec^{-1}$.

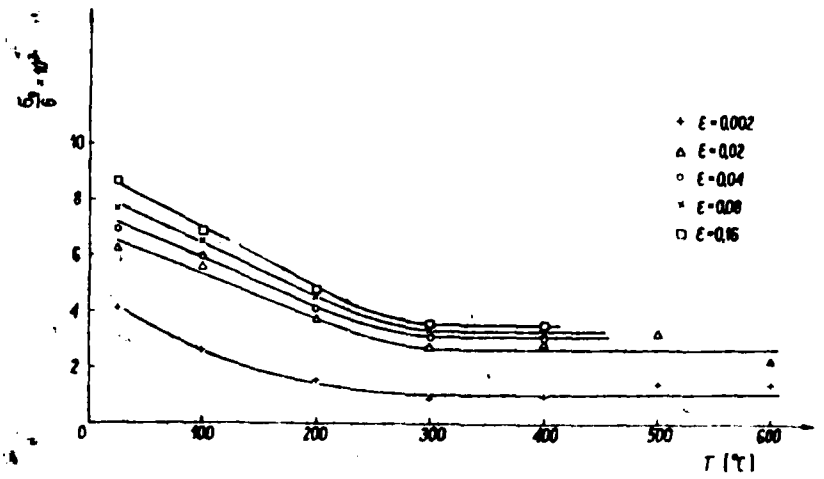

Fig 15. Temperature dependence of σ/G coefficient. Deformation speed $\dot{\epsilon} = 3.6 \times 10^{-4} sec^{-1}$.

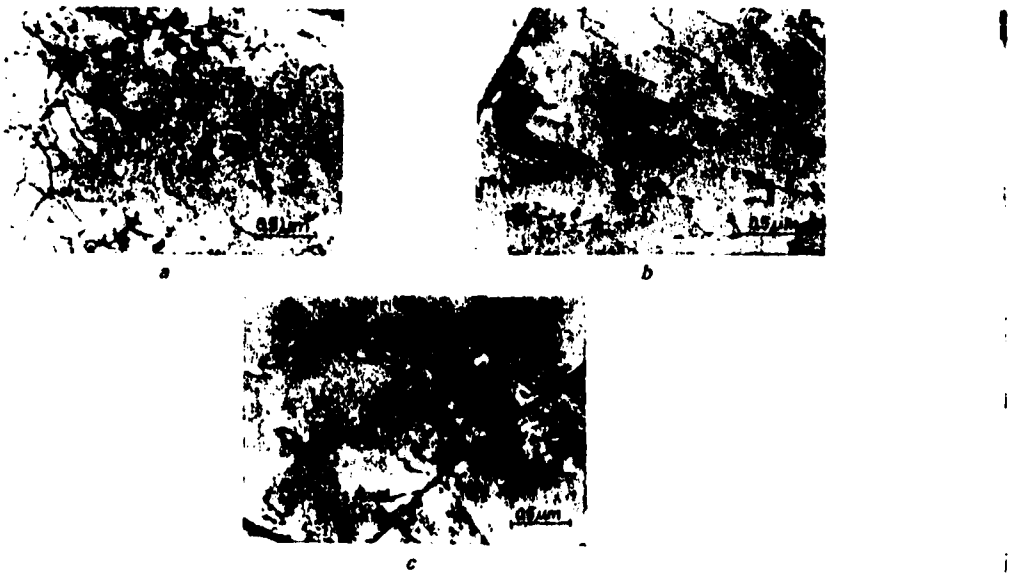

Fig 16. Structure of alpha titanium with the grain size of 8.7 μm, ϵ= 0.01 deformation at 25°C.

Fig. 17

Fig. 18

Fig 17. Structure of alpha titanium with the grain size of 0.7 μm. ϵ = 0.02 deformation at 300° C.

Fig 18. Structure of alpha titanium with the grain size 170 μm, ϵ = 0.01 deformation, at 25° C.

Fig 19. Structure of alpha titanium with the grain size 170.0 μm, ε = 0.02 deformation, at 300°C.

Fig 20. The grain boundary in alpha titanium after microdeformation.

Fig. 21

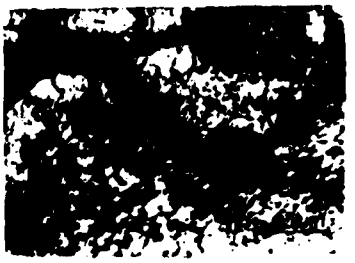

Fig. 22

Fig 21. Structure of alpha titanium with the 8.7 μm grain size, ε = 0.04 deformation, at 25° C.

Fig 22. Structure of alpha titanium with the 8.7 μm grain size, ε = 0.06 deformation, at 25° C.

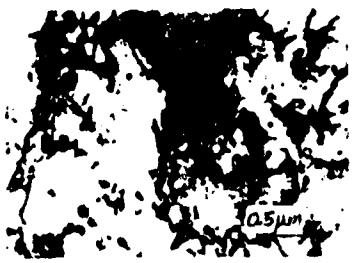

Fig. 23

Fig. 24

Fig 23. Structure of alpha titanium with 5.7 μm grain size, ϵ = 0.04 deformation at 300° C.

Fig 24. Structure of alpha titanium with the 170.0 μm grain size, ϵ = 0.04 deformation at 300° C.

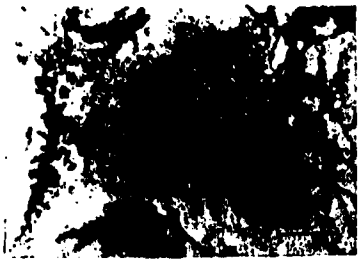

Fig. 25

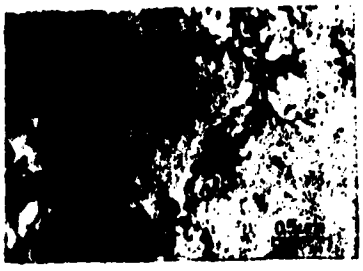

Fig. 26

Fig 25. Structure of alpha titanium with 5.7 μm the grain size, ϵ = 0.06 deformation at 300° C.

Fig 26. Structure of alpha titanium with 170.6 μm grain size, ϵ = 0.06 deformation at 300° C.

DISTRIBUTION LIST

DISTRIBUTION DIRECT TO RECIPIENT

ORGANIZATION		MICROFICHE
A205	DMATC	1
A210	DMAAC	2
B344	DIA/RDS-3C	9
C043	USAMIIA	1
C509	BALLISTIC RES LABS	1
C510	AIR MOBILITY R&D LAB/FIO	1
C513	PICATINNY ARSENAL	1
C535	AVIATION SYS COMD	1
C591	FSTC	5
C619	MIA REDSTONE	1
D008	NISC	1
H300	USAICE (USAREUR)	1
P005	DOE	1
P050	CIA/CRB/ADD/SD	1
NAVORDSTA (50L)		1
NASA/KSI		1
AFIT/LD		1
LLL/Code L-389		1

ORGANIZATION		MICROFICHE
E053	AF/INAKA	1
E017	AF/RDXTR-W	1
E403	AFSC/INA	1
E404	AEDC	1
E408	AFWL	1
E410	ADTC	1
	FTD	
	CCN	1
	ASD/FTD/NIIS	3
	NIA/PHS	1
	NIIS	2